Special soliton structures in the (2+1)-dimensional nonlinear Schrödinger equation with radially variable diffraction and nonlinearity coefficients

Wei-Ping Zhong,[1,2,*] Milivoj R. Belić,[2] and Yuzhou Xia[3]
[1]*Department of Electronic and Information Engineering, Shunde Polytechnic, Guangdong Province, Shunde 528300, People's Republic of China*
[2]*Texas A & M Univsersity at Qatar, P.O. Box 23874, Doha, Qatar*
[3]*School of Information Science and Engineering, Southeast University, Nanjing 211189, People's Republic of China*
(Received 25 September 2010; revised manuscript received 14 December 2010; published 14 March 2011)

Applying Hirota's binary operator approach to the (2+1)-dimensional nonlinear Schrödinger equation with the radially variable diffraction and nonlinearity coefficients, we derive a variety of exact solutions to the equation. Based on the solitary wave solutions derived, we obtain some special soliton structures, such as the embedded, conical, circular, breathing, dromion, ring, and hyperbolic soliton excitations. For some specific choices of diffraction and nonlinearity coefficients, we discuss features of the (2+1)-dimensional multisolitonic solutions.

DOI: 10.1103/PhysRevE.83.036603 PACS number(s): 05.45.Yv, 42.65.Tg

I. INTRODUCTION

Soliton theory supplies ample applications to various fields of natural sciences, such as plasmas physics, hydrodynamics, nonlinear optics, fiber optics, solid state physics, and others [1]. Interactions between solitons play an important role in soliton theory. Solitary waves in (1+1) dimensions have been studied extensively, and are understood quite well, both in theoretical and experimental aspects [1]. In (2+1) and higher dimensions the situation is less clear. Some significant integrable models have been established in nonlinear (NL) physics [2–5], involving the evolution partial differential equations (PDEs). In (2+1) dimensions [(2+1)D], NL evolution equations possess richer solutions than in (1+1)D, and from the study of (2+1)D models it is known that in higher dimensions there exist more abundant symmetric structures than in the lower dimensions. Different special types of localized solutions of the (2+1)D integrable models have been obtained by means of different integration methods. Especially, one type of coherent soliton solutions, called the dromions, first introduced by Boiti [5], has attracted much attention. They travel on the intersections of the plane solitons of an auxiliary field and generally decay exponentially in all spatial directions.

In recent years, several significant (2+1)D and (3+1)D models, described by different multidimensional NL equations, such as the Kadomtsev-Petviashvili [2], Davey-Stewartson [3], the generalized Korteweg-de Vries [6], asymmetric Nizhnik-Novikov-Vesselov [4], sine-Gordon [7], breaking soliton [8], scalar NL Schrödinger [9], Korteweg-de Vries in (3+1)D [10], and Jimbo-Miwa-Kadomtsev-Petviashvili [11] equations, have been intensively investigated. Different types of localized solutions to these models have been obtained, using different approaches. These approaches include the bilinear method [12], the inverse scattering transformation [13], Backlund and Darboux transformations [14], and the homogeneous balance and *F*-expansion technique [15,16], among others. From the above studies of (2+1)D and (3+1)D models, it became obvious that there exists a much greater variety of localized structures in higher dimensions than in the lower dimensions. This fact hints at the existence of new localized structures that are still unrevealed in many of the multidimensional NL integrable models. We uncover such solutions in the NL Schrödinger equation with varying coefficients.

In this paper we introduce a special analytical stationary solution form, composed of two specific spatial functions, of the (2+1)D NL Schrödinger equation (NLSE) with radially variable diffraction and nonlinearity coefficients. A system of two equations is obtained for the four functions, i.e., the diffraction coefficient, the nonlinearity coefficient, and the two assumed solution functions. Different spatially variable diffraction and NL coefficients can be constructed when explicit solutions of the NLSE are assumed, leading to many kinds of three-dimensional (3D) localized structures. Such localized modes might be useful in explaining some phenomena in both Bose-Einstein condensates and NL optical systems. The stability of these 3D localized excitation structures will be studied elsewhere.

It should be mentioned that the stability of localized solutions to the multidimensional NL evolution PDEs is still an open problem. Lately, much progress has been achieved by the introduction of dispersion (or diffraction) and nonlinearity management techniques [17].

This paper is organized as follows. In Sec. II we briefly outline the main steps of our analytic solution method and apply this method to the NLSE system with radially variable coefficients. In Sec. III we discuss different structures that are obtained using the method. A simple summary is given in the final section.

II. MODEL AND THE SOLUTION METHOD

We describe the propagation of a light beam along the z axis in a Kerr medium, using the scaled NLSE with radially variable diffraction and nonlinearity coefficients, for the complex field amplitude u:

$$i\frac{\partial u}{\partial z}+\frac{1}{2}\beta(r)\nabla_{\perp}^{2}u+N(r)|u|^{2}u=0, \tag{1}$$

where $\beta(r)$ and $N(r)$ are the variable diffraction and nonlinearity coefficients, respectively. Here $\nabla_{\perp}^{2}$ is the

*zhongwp6@126.com

transverse Laplacean operator expressed in polar coordinates, $r=\sqrt{x^2+y^2}$ is the transverse distance, and φ is the azimuthal angle. We presume a solution that separates the variables in polar coordinates, (r,φ), and look for the solutions of Eq. (1) in the form $u(r,\varphi,z)=\phi(\varphi)U(r,z)$. We assume that the azimuthal part of the solution is of the form [18] $\phi(\varphi)=\cos(m\varphi)+iq\,\sin(m\varphi)$, where m is a non-negative real constant—the so-called topological charge (TC). Usually, TC is assumed to be an integer, but it could also be fractional, allowing the possibility of fractional angular momentum; such a possibility has been discussed theoretically [19] and demonstrated experimentally [20]. The parameter $q\in[0,1]$ determines the modulation depth of the beam intensity. Note that the azimuthal part is only an *approximate* solution of Eq. (1), valid for weak nonlinearity or large values of q; this is because the $|u|^2$ term in the nonlinearity retains the φ dependence and spoils the separation of variables.

Inserting the ansatz for $u(r,\varphi,z)$ into Eq. (1), integrating over φ from 0 to 2π, and when m is an integer or half-integer, one readily derives an *averaged* equation for U:

$$i\frac{\partial U}{\partial z}+\frac{1}{2}\beta(r)\left(\frac{\partial^2}{\partial r^2}+\frac{1}{r}\frac{\partial}{\partial r}-\frac{m^2}{r^2}\right)U+\frac{1}{2}N(r)(1+q^2)|U|^2U=0. \tag{2}$$

We define the complex field $U(z,r)$ of Eq. (2) in terms of its amplitude A and phase B [16,18], $U(z,r)=A(r)e^{iB(r)+i\mu_0 z}$, where μ_0 is the propagation constant of the beam. Substituting $U(z,r)$ into Eq. (2) and separating the real and imaginary parts yields two coupled equations,

$$-\mu_0A+\frac{1}{2}\beta\left[\frac{\partial^2A}{\partial r^2}-A\left(\frac{\partial B}{\partial r}\right)^2+\frac{1}{r}\frac{\partial A}{\partial r}-\frac{m^2}{r^2}A\right]+\frac{1}{2}N(1+q^2)A^3=0, \tag{3a}$$

$$2\frac{\partial A}{\partial r}\frac{\partial B}{\partial r}+A\frac{\partial^2B}{\partial r^2}+\frac{1}{r}\frac{\partial B}{\partial r}A=0. \tag{3b}$$

In general, this system of equations is difficult to handle analytically. However, by assuming a relation between the phase and the amplitude $\frac{\partial B}{\partial r}=\frac{\lambda}{rA^2}$, Eq. (3b) is turned into an identity. Such a relation, to our knowledge not mentioned in the literature before (at least not for $\lambda\neq0$), testifies about the novelty of the solutions obtained. Here λ is an arbitrary constant of integration. In this paper we consider only the solutions of this type. Equation (3a) now becomes

$$\beta\left(A^3\frac{\partial^2A}{\partial r^2}+\frac{1}{r}A^3\frac{\partial A}{\partial r}-\frac{m^2}{r^2}A^4\right)+N(1+q^2)A^6-2\mu_0A^4-\frac{\lambda^2}{r^2}=0. \tag{4}$$

The treatment of Eq. (4) is advanced by the introduction of Hirota's binary operator [12,21], $D_r[g(r)f(r)]=(\frac{\partial}{\partial r}-\frac{\partial}{\partial r'})g(r)f(r')|_{r=r'}$. We assume that the amplitude A can be represented as a quotient $A=\frac{g}{f}$, where f and g are real functions of the real positive argument r. Naturally, they are assumed nonzero. Then Eq. (4) can be expressed in the form of two bilinear Hirota forms for $N(r)$ and $\beta(r)$:

$$N(r)=\frac{(2r^2g^4\mu_0+\lambda^2f^4)fD_r^2(ff)}{g^5\left[m^2gf(1+q^2)-(1+q^2)r^2D_r^2(gf)-(1+q^2)rD_r(gf)\right]},] \tag{5a}$$

$$\beta(r)=N(r)\frac{(1+q^2)g^2}{D_r^2(ff)}. \tag{5b}$$

At this point it is convenient to recall the form of the *approximate analytical* solution of Eq. (1):

$$u(r,\varphi,z)=(\cos m\varphi+iq\,\sin m\varphi)\frac{g}{f}e^{iB(r)+i\mu_0z}, \tag{6}$$

where $B(r)=\lambda\int\frac{f^2}{rg^2}dr+B_0$. Thus, the free parameter λ parametrizes the phase B and the coefficients N and β through Eq. (5). It does *not* parametrize directly the amplitude A, although it figures explicitly in Eq. (4); A is determined only by the ratio $\frac{g}{f}$. In the specific examples below we take $\lambda=1$ and $\mu_0=1$.

Arbitrariness in the choice of functions g and f included in the above solution (6) implies that the beam field $u(z,r,\varphi)$ may possess a rich structure. The freedom in the solution of Eqs. (5a) and (5b) makes it feasible to consider an *inverse* problem: First, give appropriate expressions of g and f to describe the desired NL localized modes, and then obtain the corresponding $N(r)$ and $\beta(r)$, which produce such solutions. This feature is both a blessing and curse of the procedure: It opens a way to find analytical solutions to different NLSEs, but also opens a path to the production of pairs of weird solutions to weird equations of little physical relevance. While at first sight the procedure may look as finding solutions in search of a problem, that really is not so: The initial Eq. (1) is a well-defined physical model with a wealth of applications in different fields of physics, and a careful choice of g and f may lead to viable models with realistic nonlinearity and diffraction coefficients. In addition, one may use information acquired on $N(r)$ and $\beta(r)$ not only for engineering purposes—to model novel materials—but, by simplifying usually complex analytical form of these coefficients, to consider the effect on the numerical solutions of Eq. (1). Following this route, we construct some interesting exact solutions possessing localized NL structures with $N(r)$ and $\beta(r)$ determined by Eqs. (5a) and (5b). A general constraint is that when $r\to\infty$, $|u|$ should approach zero; namely, it should be a localized solution. However, we also include solutions where $|u|$ approaches a constant. Such solutions are more difficult to justify physically,

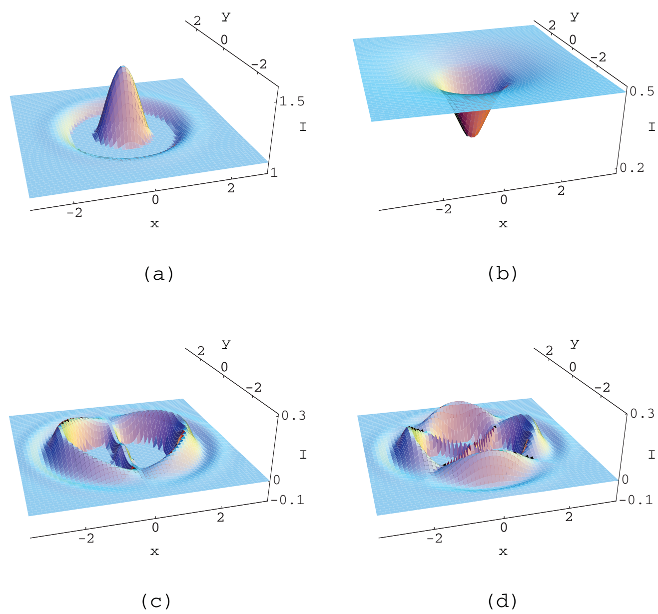

FIG. 1. (Color online) Special soliton structures for different f and g. The amplitude distribution $|u|$ is presented for the functions and parameters specified in the text. (a), (b) Embedded solitons. (c), (d) Circular solitons.

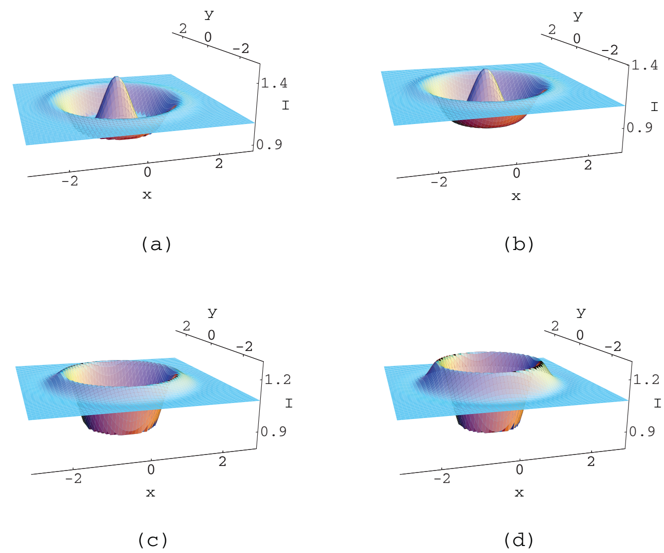

FIG. 3. (Color online) Distribution plots of the amplitude of a parametric breather. Other parameters are as in the text.

but are relevant, for example, in situations where a localized solution, bright or dark, is riding on a broad carrier wave or on a continuous wave background [22].

III. NONLINEAR LOCALIZED EXCITATIONS

In this section we introduce some special types of localized excitations for the scalar field u expressed by Eq. (6) via suitable selections of the arbitrary functions f and g. We focus attention on the distributions of the amplitude $I = |u|$. The diffraction and nonlinearity coefficients corresponding to the functions f and g are calculated from Eqs. (5). In general, exact expressions for $N(r)$ and $\beta(r)$ are likely to be of some unusual and complex form, therefore, we do not provide them.

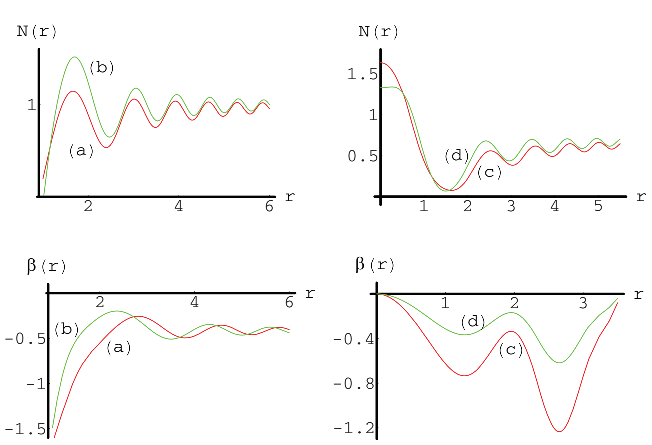

FIG. 2. (Color online) Graphs of the diffraction and nonlinearity coefficients corresponding to Fig. 1.

However, we provide the graphs of $N(r)$ and $\beta(r)$. The point is that one can use these graphs, as well as analytical expressions, to introduce similar but simpler forms of the coefficients that could help in designing physically viable material models and allow numerical treatment of Eq. (1) with assured existence of localized solutions. All the examples in this section are valid for the general model given by Eq. (1), within assumptions presumed above and without additional constraints.

A. Embedded soliton excitations

If the functions f and g are chosen as

$$g = \cosh(\chi) + 1, \quad f = \sinh(\chi), \tag{7}$$

and the function $\chi(r)$ is arbitrary, various structures are obtained. We call such excitations the embedded solitons; the name first appeared in Ref. [23]. An example is presented in Fig. 1(a) for the function $\chi = \frac{1}{1+\exp(-r^2)\cos(r^2-a)}$, where a is a constant and $q = 1$. In that figure, $a = 11.5$. Similarly, we can construct a conical dark soliton excitation for $\chi = \frac{1}{1+\exp(-r^2)\cos(r^2)}$, i.e., for $a = 0$ and $q = 1$; this soliton distribution is presented in Fig. 1(b). Reference [24] mentions conical dark solitons, but in a different context.

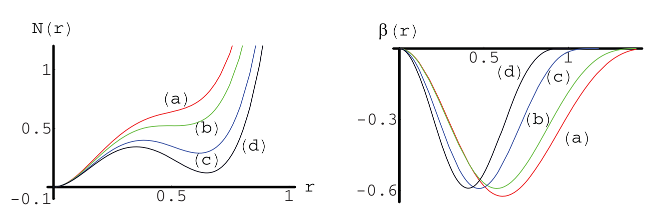

FIG. 4. (Color online) Diffraction and nonlinearity coefficients corresponding to Fig. 3.

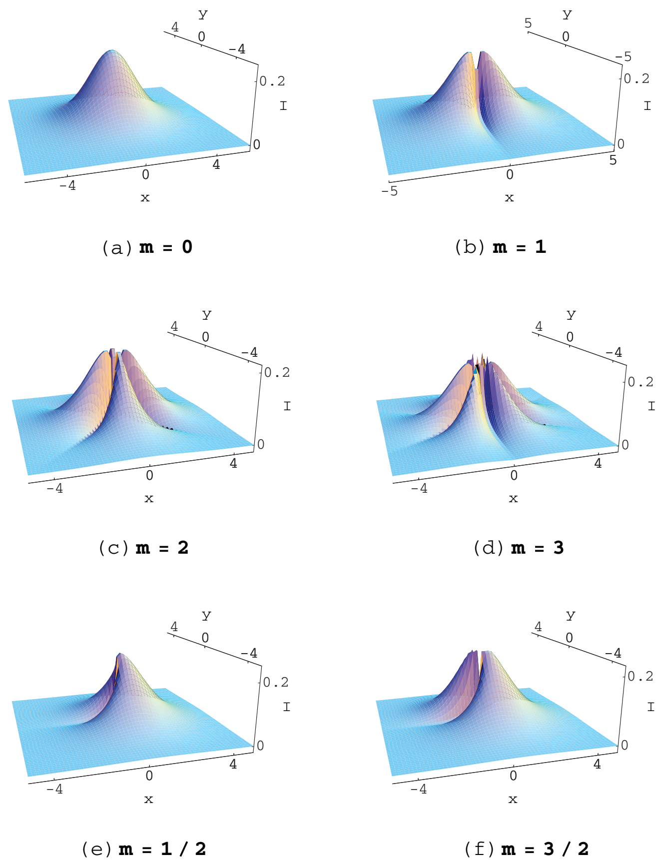

FIG. 5. (Color online) Single and multiple dromion excitations with $q = 0$, for different TCs.

B. Circular soliton excitations

To obtain more of the special solitary structures, we choose $g = \sin(r^2 + \pi)$, $f = \exp(\frac{r^2}{2})$, with $q = 0.9$ and different values of m. Localized solutions are also modulated by the function $\sin(r^2 + \pi)$; Figs. 1(c) and 1(d) show the structures of a circular soliton for the parameters $m = 1$ and $m = 2$ in Figs. 1(c) and 1(d), respectively. Similar circular solitons have appeared in Ref. [25], in the numerical solution of the sine-Gordon equation.

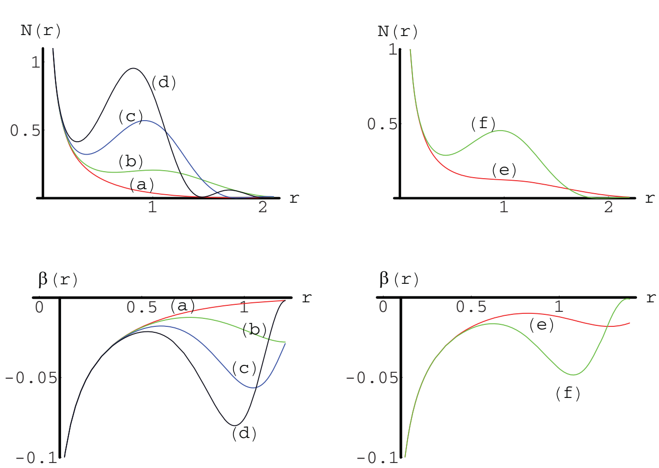

FIG. 6. (Color online) Diffraction and nonlinearity coefficient functions corresponding to Fig. 5.

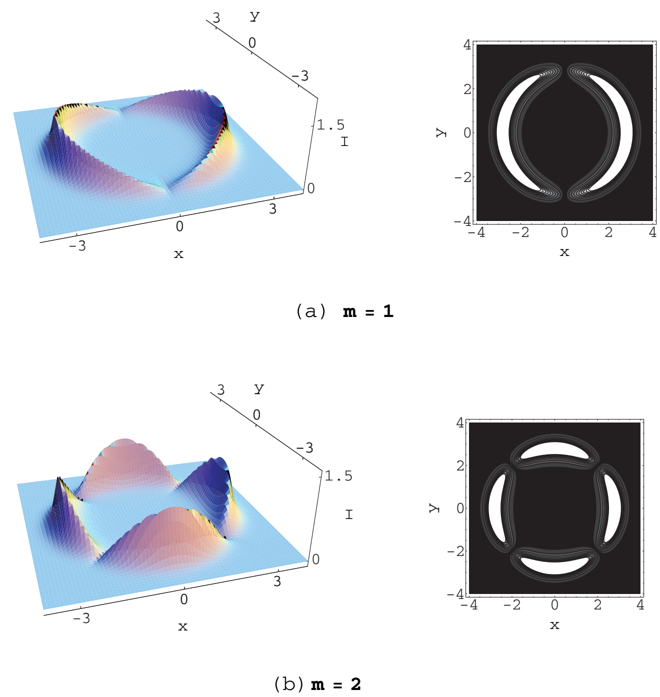

FIG. 7. (Color online) Ring soliton structures. The amplitude distribution is shown on the left-hand side and the contour plot on the right-hand side. Other parameters are given in the text.

The diffraction and nonlinearity coefficients corresponding to the functions f and g given by Eq. (7) are shown in Fig. 2. Because g and f contain the periodic modulation, coming from $\sin(r^2 + \pi)$ or $\cos(r^2 - a)$, the diffraction and nonlinearity coefficients show oscillations. We find that when r is small, owing to the impact of the exponential function, $N(r)$ and $\beta(r)$ decrease rapidly and then tend to a constant. Among actual physical systems, materials with positive and/or negative nonlinearity and negative modulated diffraction can be found, for example, among the left-handed materials. Also, in the related models describing light bullets [26] and solitary pulses [27], when the second-order *time* derivative appears in the Laplacean of Eq. (1), the corresponding *dispersion* coefficient can commonly assume negative values.

C. Parametric breather excitations

Breather solutions in the (1+1)D case present a type of common and important nonlinear excitation [1]. Because of the arbitrariness of the functions f and g in Eq. (6), the breather solutions of the (2+1)-dimensional NLS model

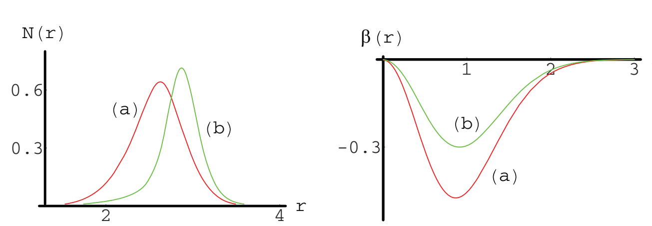

FIG. 8. (Color online) The variable diffraction and nonlinearity coefficients of the ring solitons from Fig. 7.

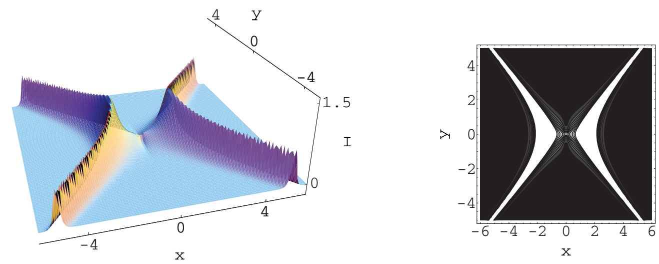

(a) **m = 1**

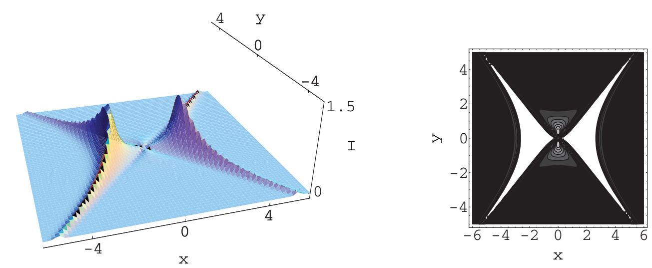

(b) **m = 2**

FIG. 9. (Color online) Hyperbolic soliton excitations. Figure setup is as in Fig. 7. The parameter $q = 1$ and other parameters are given in the text.

display quite a rich structure. We present only one example of the parametric type of breathers, with the selection $\chi = 1 + \text{sech}(-r^2)\sin(r^2 + \rho)$ in Eq. (7) and with $q = 1$; here ρ is an arbitrary constant. Note that the breathing here denotes the change in the intensity profile as the parameter ρ is varied, and not the change as the structure propagates. From the expressions in Eqs. (6) and (7) it is evident that these types of parametric breathers may "breathe" in different ways. For instance, they may breathe in their amplitudes, radii, or positions. An example is provided in Fig. 3, where the parameter ρ is taken as -0.2, -0.1, 0.8, and 1.5 in Figs. 3(a)–3(d), respectively. Actually, the formation of a breather is the result of the periodic modulation function $\sin(r^2 + \rho)$. The corresponding $N(r)$ and $\beta(r)$ functions are displayed in Fig. 4.

D. Dromion soliton excitations

In general, the multidromion solutions denote solutions that exponentially decay in all directions. They are driven by multiple straight linear ghost solitons with some suitable dispersion relations [9], and the dromions are located at the cross points of the straight line solitons. We take the functions g and f in Eq. (6) as $g = e^r$, $f = (1 + e^r)^2$, and $q = 0.95$. Figure 5 shows the beam amplitude $I = |u|$ of the single and multidromions.

When $m = 0$, the corresponding dromion profile is presented in Fig. 5(a). For $m \neq 0$, we observe modulated nonlinear localized excitations. In Figs. 5(b)–5(d) we present examples of symmetric excitations for $m = 1,2,3$. When m is an integer, the localized excitation contains $2m$ spots. When $m > 0$ is a half-integer, asymmetric localized excitations are obtained. Figures 5(e)–5(f) display simple asymmetric excitations, for $m = 1/2$ and $m = 3/2$. Figure 6 depicts the corresponding diffraction and nonlinearity coefficients. $\beta(r)$ is negative everywhere, while $N(r)$ is positive.

E. Ring and hyperbolic soliton excitations

Other interesting cases include the ring and hyperbolic soliton excitations. The g and f functions for the ring solitons are of the form

$$g = 1, \quad f = \cosh(\mathrm{r}^2 + \rho), \tag{8}$$

where ρ is an arbitrary constant. Ring beams are shaped as rings whose thickness is much smaller than their radius and whose intensity is azimuthally modulated for $m > 0$. The amplitude tends to develop dips and peaks around the ring, as displayed in Fig. 7 for different TCs, $q = 0.96$ and $\rho = 1$.

For $m = 0$, a uniform ring solution is obtained. Ring necklace solutions are excited for $m \geqslant 1$ an integer. Generally speaking, the NL ring excitations exhibit $2m$ dip regions and $2m$ peak regions for $m \geqslant 1$ as an integer, and they form symmetric structures. In Fig. 8 we illustrate the form of the diffraction and nonlinearity coefficients. Ring necklace solitons are common excitations in NLSEs [28].

The hyperbolic soliton excitations are obtained with the following selection of the g and f functions:

$$g = r\,\text{sech}(-r^2 + \rho), \quad f = 2 - \text{sech}(-r^2 + \rho). \tag{9}$$

Examples are shown in Fig. 9. In Fig. 10, we again illustrate the structure of the variable diffraction and nonlinearity coefficients. In Bose-Einstein condensates, which might be proper media for observation of excitations described here, typical examples that can be used to create a lower-dimensional condensate can be found in Ref. [29].

IV. CONCLUSION

In conclusion, we have constructed special exact solutions of the (2+1)-dimensional NL Schrödinger equation with variable nonlinearity and diffraction coefficients. A solution procedure is introduced, in which the nonlinearity coefficient $N(r)$ and the diffraction coefficient $\beta(r)$ expressed using Hirota's satisfy the Hirota bilinear forms, given in terms of two arbitrary functions f and g, comprising the amplitude of the solution. A number of specific variable nonlinearity and diffraction coefficients that support explicit 3D localized excitations are constructed. Various types of special solutions are presented, with different forms of the localized modes, together with the corresponding coefficients.

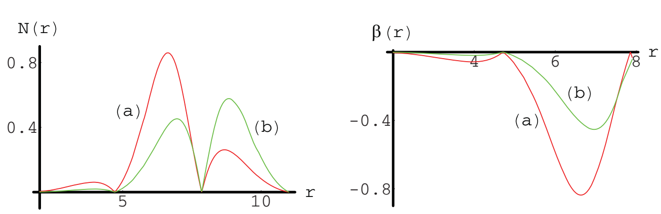

FIG. 10. (Color online) Diffraction and nonlinearity coefficients of hyperbolic soliton excitations from Fig. 9.

ACKNOWLEDGMENTS

This work is supported by the Natural Science Foundation of Guangdong Province under Grant No. 1015283001000000, China, and work at the Texas A & M University at Qatar is supported by the NPRP 25-6-7-2 and NPRP 09-462-1-074 projects with the Qatar National Research Foundation.

[1] Yu. S. Kivshar and B. A. Malomend, Rev. Mod. Phys. **61**, 763 (1989); Yu. S. Kivshar and G. P. Agrawal, *Optical Solitons: From Fibers to Photonic Crystals* (Academic, San Diego, 2003).
[2] B. B. Kadomtsev and V. I. Petviashvili, Dokl. Akad. Nauk SSSR **192**, 753 (1970) [Sov. Phys. Dokl. **15**, 539 (1970)].
[3] A. Davey and K. Stewartson, Proc. R. Soc. London, Ser. A **338**, 101 (1974).
[4] S. P. Novikov and A. P. Veslov, Physica D **18**, 267 (1986).
[5] M. Boiti, J. J. P. L'eon, L. Martina, and F. Pempinelli, Phys. Lett. A **132**, 432 (1988).
[6] R. Radha and M. Lakshmanan, J. Math. Phys. **35**, 4746 (1994).
[7] B. G. Konopelchenko and C. Rogers, Phys. Lett. A **158**, 391 (1991); J. Math. Phys. **34**, 214 (1993).
[8] R. Radha and M. Lakshmanan, Phys. Lett. A **197**, 7 (1995).
[9] R. Radha and M. Lakshmanan, J. Phys. A **38**, 3229 (1997).
[10] S. Y. Lou, Phys. Scr. **65**, 7 (2002).
[11] H. Y. Ruan and S. Y. Lou, J. Math. Phys. **38**, 3123 (1997).
[12] R. Hirota, Phys. Rev. Lett. **27**, 1192 (1971).
[13] P. A. Clarkson and M. D. Kruskal, J. Math. Phys. **30**, 2201 (1989).
[14] V. B. Matveev and M. A. Salle, *Darboux Transformations and Solitons* (Springer, Berlin, 1991).
[15] W. P. Zhong, R. H. Xie, M. Belić, N. Petrović, and G. Chen, Phys. Rev. A **78**, 023821 (2008); W. P. Zhong and M. Belić, Phys. Rev. E **81**, 056604 (2010).
[16] M. Belić, N. Petrović, W. P. Zhong, R. H. Xie, and G. Chen, Phys. Rev. Lett. **101**, 123904 (2008); W. P. Zhong and M. Belić, Phys. Rev. E **81**, 016605 (2010).
[17] B. A. Malomed, *Soliton Management in Periodic Systems* (Springer, Berlin, 2006).
[18] W. P. Zhong and L. Yi, Phys. Rev. A **75**, 061801(R) (2007).
[19] M. V. Berry, J. Opt. A **6**, 259 (2004); I. V. Basistiy, V. A. Pas'ko, V. V. Slyusar, M. S. Soskin, and M. V. Vasnetsov, *ibid.* **6**, S166 (2004).
[20] W. M. Lee, X. C. Yuan, and K. Dholakia, Opt. Commun. **239**, 129 (2004); J. Leach, E. Yao, and M. J. Padget, New J. Phys. **6**, 71 (2004); S. H. Tao, X. C. Yuan, J. Liu, X. Peng, and H. B. Niu, Opt. Express **13**, 7726 (2005).
[21] W. P. Zhong and H. Luo, Chin. Phys. Lett. **8**, 577 (2000).
[22] W. N. Cui, C. L. Sun, and G. X. Huang, Chin. Phys. Lett. **20**, 246 (2003).
[23] A. A. Minzoni, N. F. Smyth, and A. L. Worthy, Physica D **206**, 166 (2005).
[24] T. L. Horng, S. C. Gou, T. C. Lin, G. A. El, A. P. Itin, and A. M. Kamchatnov, Phys. Rev.A **79**, 053619 (2009).
[25] M. Dehghan and D. Mirzaei, Comput. Methods Appl. Mech. Eng. **197**, 476 (2008).
[26] B. A. Malomed, D. Michalache, F. Wise, and L. Torner, J. Opt. B Quantum Semiclassical Opt. **7**, R53 (2005).
[27] G. P. Agrawal, *Nonlinear Fiber Optics* (Academic, Burlington, 2007).
[28] A. S. Desyatnikov and Y. S. Kivshar, Phys. Rev. Lett. **87**, 033901 (2001).
[29] A. Görlitz, J. M. Vogels, A. E. Leanhardt, C. Raman, T. L. Gustavson, J. R. Abo-Shaeer, A. P. Chikkatur, S. Gupta, S. Inouye, T. Rosenband, and W. Ketterle, Phys. Rev. Lett. **87**, 130402 (2001).